Clim. Past Discuss., 9, 6125–6160, 2013
www.clim-past-discuss.net/9/6125/2013/
doi:10.5194/cpd-9-6125-2013

Climate of the Past
Discussions
Open Access

Late Glacial-Holocene climatic transition record at the Argentinian Andean piedmont between 33–34° S

A. E. Mehl and M. A. Zárate

Instituto de Ciencias de la Tierra y Ambientales de La Pampa (INCITAP, CONICET), Universidad Nacional de La Pampa, Uruguay 151, Santa Rosa, La Pampa, Argentina

Received: 31 July 2013 – Accepted: 1 October 2013 – Published: 31 October 2013

Correspondence to: A. E. Mehl (adrianamehl@gmail.com)
and M. A. Zárate (mzarate@exactas.unlpam.edu.ar)

Published by Copernicus Publications on behalf of the European Geosciences Union.

Late Glacial-Holocene climatic transition

A. E. Mehl and M. A. Zárate

Abstract

The Arroyo La Estacada (∼33°28′ S, 69°02′ W), eastern Andean piedmont of Argentina, cuts through an extensive piedmont aggradational unit composed of a dominant late Pleistocene–early Holocene (LP–EH) alluvial sequence including several paleosols. The arroyo sedimentary record exhibits a paleosol developed affecting the topmost part of likely Lateglacial aeolian deposits aggraded into a floodplain environment by the end of the late Pleistocene. The paleosol shows variable grade of development in the outcrops along the arroyo probably in relation to fluvial valley paleotopography. Organic matter humification, carbonate accumulation and redox processes were the dominant processes associated with paleosol formation. By the early Holocene, when the formation of the paleosol ended, alluvial aggradation renewed and a higher frequency of flooding events could have affected the arroyo's floodplain environment.

A period of relative landscape stability in the Arroyo La Estacada basin is inferred from the paleosol developed by the LP–EH transition in response to a climatic amelioration in the Andes cordillera piedmont after the Late Glacial arid conditions. The renewal of early Holocene alluvial aggradation was probably influenced by the South American Monsoon and resulted in a change in the sedimentary dynamics of the arroyo.

The analyzed Late Glacial-Holocene alluvial record of the Andean piedmont constitutes a suitable record of the LP–EH climatic transition at the extra Andean region of Argentina. It is in agreement with regional paleoclimatic evidence along the southern tip of the South American continent, where other sedimentary sequences record similar late Quaternary paleoenvironmental changes over both fluvial and interfluvial areas.

CPD
9, 6125–6160, 2013

1 Introduction

The understanding of Earth's past climatic evolution is considered the key to get a better understanding of the present day climatic system and the development of longterm climatic change forecasts (Saltzman, 2002). In particular, since the Last Glacial Maximum (LGM) the ice sheet retreat and the amelioration of climate leading to our present climate conditions have not been uniform processes (Saltzman, 2002).

In South America, as well as in North America and Eurasia, the final ice sheet retreat to their present day position may have occurred about 10 kyr ago marking the beginning of the present Holocene interglacial epoch (Saltzman, 2002; Coronato and Rabassa, 2007). Specifically, in the southern tip of the South American continent the Late Quaternary paleoclimatic conditions have been mainly revealed by the glacial dynamic in the Andes Cordillera (Clapperton, 1993; Espizua, 1993, 1998, 1999; Coronato and Rabassa, 2007; Rabassa, 2008). More recently, during the last decade there has been increasing interest in Late Quaternary paleoenvironmental and paleoclimatic conditions of the extra Andean region of central Argentina. As a result, researches have been focussed on the analysis of different and varied proxies (Villalba, 1990; Prieto, 1996; Piovano et al., 2002; Zárate and Paéz, 2002; Prieto et al., 2003; Kemp et al., 2006; Boninsegna et al., 2009; Rojo et al., 2012; Navarro, 2012). Specially, the study of buried paleosols has been concentrated in the loess sequences that dominate the Pampean region, where the largest loessic plain of South America develops with a nearly 50 m thick loess record (Fig. 1a). In fact, the eastern region of the Pampean plain has been a classic area to analyse Quaternary argentinean paleosols (Teruggi and Imbellone, 1987; Imbellone and Teruggi, 1993; Blasi et al., 2001; Zárate et al., 2002; Kemp et al., 2004b; Imbellone and Cumba, 2003, among others). Also, some studies were conducted in the loess-paleosol sequence of Northwestern Argentina with the aim of inferring paleoenvironmental conditions during the late Pleistocene and early Holocene (Kemp et al., 2003, 2004a) (Fig. 1a). In spite of this, loess deposits of Argentina commonly lack stratigraphical resolution to analyze the approximately last

CPD
9, 6125–6160, 2013

14 kyr paleoclimatic–paleoenvironmental conditions (Zárate et al., 2000). As a consequence, and taking into account the large potential of South American fluvial systems for paleoclimatic research (Baker, 2000; Zárate et al., 2000; Latrubesse, 2003), many studies have been concentrated in the analysis of alluvial sequences of the Pampean plain (Fidalgo et al., 1973; Zárate et al., 2000; Prieto et al., 2004; Quattrocchio et al., 2008; Zech et al., 2009). Some of them combine information from fluvial sedimentology, pedology and biological proxies and provide all together a more compelling framework for the knowledge of Lateglacial and Holocene paleoenvironmental–paleoclimatic conditions in Argentina.

Particularly, in the piedmont of the Andes Frontal cordillera in Mendoza province, central-western Argentina, the record of the Lateglacial and Holocene climatic changes is mainly restricted to the alluvial sequences exposed in the riverbanks of the fluvial systems draining the piedmont (Fig. 1b). At the Arroyo La Estacada fluvial basin (eastern Andean piedmont, $\sim 33^{\circ}28'$ S and $69^{\circ}02'$ W) there is a well constrained and laterally traceable paleosol with a formation interval started ca. 12 cal yr BP and lasted until ca. 10.6 cal yr BP. The paleosol was developed over likely Lateglacial aeolian silty sands aggraded in the paleo-floodplain environment of the arroyo (Zárate and Páez, 2002; Mehl and Zárate, 2012). A conspicuous change in the depositional arrangement of fluvial deposits took place after the formation of this paleosol (Zárate and Mehl, 2008; Mehl and Zárate, 2012).

Results from field and micromorphological analyses of the late Pleistocene–early Holocene transition in the alluvial sequences exposed at the banks of Arroyo La Estacada are presented. The final purpose is to help with the reconstruction of paleoenvironmental and paleoclimatic conditions of the central-western Argentina during the LP–EH transition. A regional correlation with other synchronous records of the extra Andean region of southern South America is also made to contribute, at a continental-scale, to the knowledge of the Late Quaternary climatic system and its variability.

CPD
9, 6125–6160, 2013

2 Regional setting and geological background

The study area comprises the fluvial basin of Arroyo La Estacada, ∼ 33°28′ S and 69°02′ W, in Mendoza province, Argentina. The region presents an arid-semiarid climate (Burgos and Vidal, 1951; Prohaska, 1961). The mean annual temperature reaches the 12.8 °C and the ca. 200 mm average annual rainfall is mostly related to short but relatively heavy rains during the austral spring and summer seasons (Barros and Silvestri, 2002). Vegetation corresponds to the "Monte" province according to Cabrera's phytogeographical classification (1976) and is dominated by xerophytic shrublands (Roig and Martínez Carretero, 1998). Nonetheless hydrophytic communities grow where water is locally available (Rojo et al., 2012). The region is included in the South American Arid Diagonal (SAAD) (Fig. 1a), an ecotone fringe where southern-eastern area has been very sensitive to past and present atmospheric circulation changes (Abraham de Vázquez et al., 2000; Piovano et al., 2009). The SAAD, comprises a narrow belt of lands that records a moisture source of Atlantic influence towards the north and east (subtropical summer rain regime), and to the western and south-western areas a Pacific influence (mainly dominated by winter precipitations) (Bruniard, 1982; Piovano et al., 2009).

The Arroyo La Estacada drains its waters to the Tunuyán River basin (Fig. 1b), the main river of this piedmont area also receiving inputs from other minor rivers and arroyo systems. The arroyo, of meandering pattern and perennial discharge, is fed by springs located along a fault line and also by Arroyo Anchayuyo, a stream collecting water in a catchment area dominated by Tertiary deposits (Fig. 1b).

The geological setting of the study area corresponds to the piedmont of Frontal cordillera, the eastern morphostructural unit composing the Andes cordillera at this latitude (Fig. 1a and b). Frontal cordillera is formed by a Proterozoic metamorphic complex, Carboniferous Permian sedimentary rocks, a wide eruptive intrusive igneous record of Permian-Triassic age, and Quaternary volcanic rocks (Caminos, 1993; Azcuy, 1993; Llambías et al., 1993; Sruoga et al., 2005; among others). Arroyo La Estacada is

CPD
9, 6125–6160, 2013

located in the northern tip of the Tunuyán Depression, a Quaternary tectonic basin developed in the piedmont area and filled with Mid to Late Quaternary sediments (Polanki, 1963). The arroyo stream cuts the Tunuyán Depression through an extensive aggradational geomorphological unit called Regional Aggradational Plain (RAP) sensu Zárate and Mehl (2008) (Figs. 1b and 2a). The RAP is characterized by a flat and gently steepening topography dropping from near 1300 m a.s.l. at the footslope of the Frontal cordillera mountain front to around 700 m a.s.l. at the vicinity of the folded and thrusted Miocene deposits that limit the tectonic depression in its eastern part (Guadal Plateau and Piedmont Hills – *Cerrilladas Pedemontanas* –; Yrigoyen, 1993; Fig. 1b). The RAP sedimentary sequence is included in the El Zampal Formation (Zárate and Mehl, 2008), previously La Estacada and El Zampal Formations according to Polanski (1963), that would likely record at least the last 120 ka, with the oldest exposures of ca. 50 ka located along the riverbanks of the arroyos crossing the area (Toms et al., 2004; Zárate and Mehl, 2008). The arroyo La Estacada excavated a nearly 20 m deep valley in the RAP deposits followed by the aggradation of a middle-late Holocene fluvial sequence presently arranged in a fill terrace geomorphological unit (Fig. 2a).

The RAP sedimentary deposits, comprising the LP–EH transition interval, are divided into a lower and an upper stratigraphic section, LSS and USS respectively (Zárate and Mehl, 2008) (Fig. 2b). The LSS is dominantly composed of homogeneous massive sand beds laterally continuous with variable thickness resulting from fluid overflows blanketing inactive areas of sandy braided channels. Also, some hyperconcentrated flow deposits, channel lag and/or longitudinal bar deposits were inferred from the presence of lenses made up of well rounded fine to coarse rock clasts (Mehl and Zárate, 2012). The uppermost 2 m of the LSS record an homogeneous and massive fine sand to silty sand deposit of likely aeolian origin with pedological features on top giving way to a buried soil laterally traceable for nearly 12 km along the Anchayuyo and La Estacada arroyos riverbanks (Zárate and Mehl, 2008; Mehl and Zárate, 2012). The minimum interval of paleosol formation was dated from ca. 11 709–12 075 cal yr BP to ca. 10 685–11 144 cal yr BP (minimum numerical ages reported by Mehl and Zárate, 2012).

CPD
9, 6125–6160, 2013

The USS develops on top of the paleosol (Fig. 2b). Its base is dominated by horizontally laminated and massive bedded sandy silts and clayey silts of variable thickness interbedded with either thin massive, horizontally laminated or ripple cross-laminated fine sand to silty sand layers. Limnic levels are very common throughout these deposits, with the lowermost yielding a date of 10 391–10 753 cal yr BP (Mehl and Zárate, 2012). These sediments were interpreted as deposited from suspension likely blanketing inactive areas of sandy braided channels with occurrence of weak traction currents generating lower-flow-regime bed forms (Mehl and Zárate, 2012). The USS middle and upper parts show interbedded massive silty sand and sandy silt layers. Two abutting paleosols develop near the 6 m depth, the upper one dated at 8454–8968 cal yr BP (Mehl and Zárate, 2012). Also, 1.5 m below the surface a paleosol was dated at 2967–3211 cal yr BP (Zárate and Mehl, 2008). It is overlaid by a moderately to highly hardpan in turn covered by a superficial massive and loose fine aeolian sand blanket (Mehl and Zárate, 2012).

3 Methodology

Three locations were chosen to illustrate the different degree of pedological development of the ca. 10 ka paleosol along the Arroyo La Estacada basin. Fieldwork was carried out at Puente El Zampal (PEZ; 33°26′52′′ S–69°03′09′′ W) and Puente Roto study sites (PR; 33°26′25′′ S–69°03′32′′ W), both located at the riverbanks of the lower reach of Arroyo Anchayuyo (Fig. 3), that contributes its waters, together with Arroyo Guajardino, to Arroyo La Estacada. The third study site selected was Finca Gatica (FG. 33°28′12′′ S–69°02′19′′ W), located at Arroyo La Estacada (Fig. 3). A distance of 1 km exists between PR and PEZ study sites; in turn FG is 4 km and 3 km far away from both study sites respectively (Figs. 1b and 3).

The results obtained from the pedosedimentary analysis of the LP–EH transition paleosol are interpreted and discussed on the basis of sedimentological, lithofacial, stratigraphical and geochronological data already reported by Zárate and Mehl (2008) and

CPD
9, 6125–6160, 2013

A. E. Mehl and M. A. Zárate

Mehl and Zárate (2012) (Fig. 3; Tables 1 and 2). Field identifications and descriptions were conducted following the main criteria pointed out by Tucker (2003), Catt (1990) and the Soil Survey Staff (1999, 2003). Dry-sediment colors are reported according to Munsell Soil Color Chart (2000) (Table 2). Wet oxidation followed by titration with ferrous ammonium sulfate was used to determine the organic matter content (Walkley & Black method) in paleosol sediments (Table 2), using the Van Bemmelen factor (1.72) that assumes a 58 % of total organic carbon in soil organic matter. A digital calcimeter was used to determine calcium carbonate content (Table 2).

A micromorphological analysis was conducted to help with the detection of post-depositional pedological features. The PEZ study site was selected as a key section to conduct the micromorphological analysis as it shows the best development of the ca. 10 ka paleosol. The analysis was focused on the depth interval between 7.35 m to 10 m of the alluvial sequence profile (topmost paleosol part is placed approximately at a 9 m depth). On the contrary, FG study site was chosen to analyze the paleosol in a position showing a low degree of pedological development. Due to access difficulties, micromorphological analysis at the FG profile was restricted to the paleosol section of approximately 0.3 m thick, and placed at a depth of near 4.5 m in the alluvial sequence profile.

Micromorphological analysis was carried out in thin sections made from undisturbed blocks collected at convenient intervals in Kubiena tins (7 cm × 5 cm × 4 cm), then air-dried and impregnated with epoxy resine according to standard procedures (Lee and Kemp, 1992). Thin sections were described under a Nikon Eclipse E400 Pol petrological microscope with a 10–400× magnification following the terminology and criteria proposed by Bullock et al. (1985) and Catt (1990). Key micromorphological observed features (fabric, structure-microstructure, coarse/fine materials, basic components, groundmass and pedofeatures) are quantified and summarized into tables attached to Figs. 4 and 6.

CPD
9, 6125–6160, 2013

4 Results

4.1 Macroscopic features of the late Pleistocene-Holocene transition paleosol

4.1.1 Puente El Zampal study site

At PEZ study site the ca. 10 ka paleosol is 9 m below the RAP surface and 7 m above the arroyo Anchayuyo water level (Figs. 2b and 3). It exhibits an A/C profile with a thickness of nearly 0.4 m and it is characterized by a massive aspect and high firmness. When broken in the hand it has blocky appearance. Color varies downward from gray (10YR 5/1, 6/1)-light brownish gray (10YR 6/2) to light gray (10YR 7/1, 7/2) (Table 2). Organic matter decreases in the same way from 1.33 % to 0.40 % while calcium carbonate content passes downward from non-calcareous to very slightly calcareous (Table 2). Approximately 0.65 m below the paleosol there are calcitic nodules grading into calcitic mottles towards the lower levels. Numerical ages reported for this paleosol were obtained from the topmost and lowermost part of the A horizon: 10 685–11 144 cal yr BP and 11 709–12 075 cal yr BP respectively (Table 2).

4.1.2 Puente Roto study site

At this study site the paleosol is 10 m below the RAP surface and near 10 m above the arroyo Anchayuyo water level (Fig. 3). It exhibits an upper A horizon and a preliminary described Ck or Bk horizon. Faint color changes downward in a gradual way from light brownish gray (10YR 6/2) to very pale brown (10YR7/3, 8/4) (Table 1). Organic matter content reaches up to 2 % but decreases markedly toward the paleosol base (Table 1). Calcium carbonate content changes from slightly calcareous in the paleosol upper part to very calcareous in the base exhibiting calcitic nodules. Also, there are calcitic concretions at a depth of approximately 0.6 m below the paleosol (Table 1). A calibrated radiocarbon age of 11 275–11 805 yr BP was reported from the organic matter content of the paleosol topmost part (Table 2).

CPD
9, 6125–6160, 2013

4.1.3 Finca Gatica study site

At FG study site, the LP–EH paleosol is placed at a depth of 4.5 m from the RAP surface and near 15 m above the arroyo La Estacada water level. In this location, the paleosol exhibits a relative higher paleotopographic position and a poorer degree of pedological development when compared with PEZ and PR exposures (Fig. 3). It shows a thickness of 0.3 m, an A–C horizonation and a massive structure. Color changes from light brownish gray (10YR 6/2) in the paleosol upper part to very pale brown (e.g. 10YR7/3, 8/4) at the base (Table 1). Paleosol organic matter content is low showing a very little increment downward (Table 2). The same happens with calcium carbonate content resulting in a slightly calcareous paleosol base (Table 2), where some isolated powdery concentrations of calcium carbonate can be observed. The paleosol has not been dated at this place. Nonetheless its age was inferred from its position 10 m above a tephra level correlated with the 24 to 30 ka BP tephra layers dated by Toms et al. (2004) at Brazo Abandonado (33°28′13″ S and 69°02′39″ W) study site, 1.5 km downstream from FG study site.

4.2 Micromorphological aspects

4.2.1 Puente El Zampal micromorphology

The deposits immediately underlying the ca. 10 ka paleosol (Samples: PEZ 10, 11 and 12. Fig. 4) exhibit homogeneous coarse silt and sandy silt to clay sediments ($\sim C/F_{62}$: 80–20, 60–40 and 15–85) without an appreciable organic matter content and a relative dearth of bioturbation features. The matrix is characterized by a massive microstructure and a crystallitic B-fabric. Typic calcitic nodules and zones with diffuse impregnation of calcium carbonate are a common feature of these samples, occasionally associated to a spongy microstructure (Fig. 5a). There are few calcitic hypocoatings around voids. Rare clay hypo-coatings and excrements infilling voids are observed along the sections (Fig. 5b). In addition, concentrations of isotropic materials (e.g. organic matter,

CPD
9, 6125–6160, 2013

tephra, diatoms or phytoliths) could also be seen. Very few to few ferruginous features (nodules, hipo-quasicoatings and diffusion features) (Fig. 5c) are also observed.

The LP–EH transition paleosol (Samples: PEZ 8 and 9, Fig. 4) shows a sedimentary matrix dominated by sandy silt to silty sand textures ($\sim C/F_{62}$: 30–70 and 70–30, Fig. 4). The upper soil horizon, attributable to an A horizon (Sample: PEZ 8, Fig. 4), presents a weak grade of pedality and a B-fabric varying across the thin section among cross-striated, reticulate striated and unistral. Although the soil mass exhibits a general homogeneous appearance related to a massive microstructure, some thin section areas exhibit spongy microstructure linked to bioturbation features (channels and chambers, some of them showing mamillate surface walls). There are spheroid aggregates smaller than 74μ associated to voids in turn excremental features are rare. This soil horizon has common partially degraded plant residues (Fig. 5d) with a dominant random distribution. Nevertheless few root fragments are preserved inside vertical to subvertical channels. Few calcitic nodules and common cemented zones are observed along with concentrations of isotropic materials assigned to glass shards.

Although the lower C horizon (Sample: PEZ 9, Fig. 4) shows a dominant massive microstructure, scarce zones develop weak spongy microstructure (Fig. 5e). The sedimentary matrix is formed mainly by very fine sand to coarse silt grains ($\sim C/F_{62}$: 70–30). Nonetheless a mosaic-speckled B-fabric can be observed due to the presence of clays in the soil mass. Organic matter concentration is not appreciable in this soil horizon; there are common weak calcitic impregnations (> 10 %) that turn stronger in the upper and lower zone of the thin section. Also some rare calcitic hypo-coatings develop around voids and some scarce ferruginous concentrations are observed.

The 1.5 m thick sedimentary deposit resting on the LP–EH transition paleosol (Samples: from PEZ 1 to 7. Fig. 4) exhibits laminated horizontal layers with variable grain sizes (including fine sand, silt and clayey silt) and common horizontally aligned platy mica grains. Cross-striated and mosaic-specked B-fabrics dominate the sedimentary matrix, but enaulic B-fabric is also observed. Along this sedimentary sequence interval, ferruginous–manganiferous nodules and diffusion features are common to few while gypsum crystal aggregates are common in some samples (Samples: PEZ 2, 3 and 4, Fig. 5f). In general, calcitic concentrations are scarce. Although voids reach up to 40 % of the thin section surface, there are areas with a porosity of just a 2 %. Most of the voids correspond to channels and chambers. Excrements, when present, are linked to voids. Rare clay coatings are observed inside some chambers (Fig. 5g). Plant residues exhibiting a horizontal alignment, root fragments including among them, are common in some levels (Fig. 5h). Besides organic matter punctuations are common in the lower levels of this interval where common to few diatoms are also observed.

4.2.2 Finca Gatica micromorphology

At FG study site, the ca. 10 ka paleosol profile is dominated by silt to clay sediments ($\sim C/F_{62}$: 30–70; Fig. 6). Porosity varies across the paleosol reaching up to 10–15 % in the upper horizon where voids are related to vughs and channels, the latter mostly likely linked to roots. Some chambers with mamillate surface roughness are observed (Fig. 7a and b). Porosity increases to 20–25 % in the middle paleosol zone corresponding mainly to vughs and cracks (Fig. 7c), the first probably relate to soil micro-fauna activity. At the paleosol base some channels and chambers can be recognized, but porosity is in general lower than 5 %.

Calcitic concentration features are seen throughout the profile. Micrite is most abundant in the middle paleosol section and is possibly linked to water movement through the soil mass (Fig. 7c and d). In turn, at the top and base of the paleosol most of the micritic concentrations are restricted to voids (Fig. 7e), likely in relation to water passing through them or to plant roots respiration. However some rare diffusion features can be observed at this section (Fig. 7f). Typic micrite nodules appear in a small proportion (0.2–2 %) at the basal horizon.

Ferruginous and manganiferous concentration features are also present in the soil profile. The upper part has few ferruginous void hypocoatings and oxide diffusion features affecting the soil mass. They become common in the middle to lower part, where

CPD
9, 6125–6160, 2013

diffusion features are linked to almost a 70 % of the voids. Additionally, middle and lower parts exhibit few nodules and very few quasicoatings of this composition.

5 Discussion

The LGM and Lateglacial in the eastern Andean piedmont between 33–34° S and the central region of Argentina were dominated by arid conditions and aeolian sedimentation (Kemp et al., 2004, 2006; Tripaldi and Forman, 2007; Frechen et al., 2009; Tripaldi et al., 2011; Mehl and Zárate, 2012). At the Arroyo La Estacada basin an aeolian deposit of nearly 1 m thick interbedded within the late Pleistocene-Holocene alluvial sequence could be interpreted as a marker of those arid conditions (Mehl and Zárate, 2012). Its deposition was followed by the development of pedological processes affecting the topmost part of the aeolian deposits and resulting in a paleosol that records scarce pedogenetic features. The interval of relative landscape stability across the fluvial basin dates back from 11 709–12 075 cal yr BP to ca. 10 685–11 144 cal yr BP (Mehl and Zárate, 2012). Although arid conditions would have remained in the region after the Lateglacial, a slight increase in the relative atmospheric humidity and temperatures after the Lateglacial could favour the paleosol development.

Organic matter humification along with calcium carbonate accumulation expressed in the formation of nodules, concretions and paleosol cemented zones, were the dominant soil formation processes. We have not yet analyzed soil carbonate morphology and geochemistry, which will provide additional insight into carbonate genesis and associated paleoenvironmental conditions. Secondarily, processes of oxidation and reduction of iron, manganese and likely sulphurs occurred affecting not only the LP–EH transition paleosoil mass but also the overlaying paleosol deposits. At PEZ and PR study sites, paleosol features are more conspicuous than at FG study site where there is a relative dearth of pedological features making difficult its distinction in the sedimentary sequence. This variable grade of paleosol development could be probably related to a paleo-location of PEZ study site in a floodplain environment proximal to the main stream crossing the area at that time. Conversely, the PR and FG paleosol exposures were likely related to more distal and higher topographic positions in the floodplain environment.

At PEZ study site an A horizon is distinguished on the basis of higher plant residues concentration, most of them are placed in a disturbed position but others maintain growth position, e.g. roots. Bioturbation features are scarce. C horizon lacks organic matter and parent materials are dominant. Redox features are scarce in the paleosol. In turn they become abundant in the overlaying sediments, and, in minor proportion, in the underlying ones. They permit to infer poor sediment drainage stages (hydromorphic stages) indicating an excess of water for some periods. Neoformation gypsum crystals in the sediments overlaying paleosol reflect subsequent stages of likely driest conditions. Horizontally arranged organic matter accumulations in the laminated sediments above paleosol indicate the likely transport and accumulation of plant residues by fluid flows affecting the aggradational plain once pedological processes ended ca. 10 685–11 144 cal yr BP and alluvial aggradation renewed.

At FG study site the LP–EH transition paleosol is poorly developed. An A horizon with very low organic matter concentration is distinguished from a greater presence of bioturbations, by micro fauna activity, than the surrounding sediments. As a result this horizon has a high degree of porosity in comparison with lower C horizon. Although calcium carbonate concentration is low in the paleosol, calcitic nodules and micritic cementations are observed at a macroscopic and microscopic level, respectively. Chemical analysis reflects a C horizon with mildly higher organic matter content than A horizon, a feature that is not inferred in the paleosol profile outcrop where color seems lighter toward the paleosol base. This anomalous organic matter content could be related to preferential organic matter conservation along the soil profile (soil upper part more susceptible to oxidation and organic matter losses), or to a primary higher organic matter concentration in the sediments then affected by pedogenesis.

By the early Holocene, the analyzed alluvial sequence records laminated epiclastic sediments layers interbedded with highly organic content sediments indicating

CPD
9, 6125–6160, 2013

a renewal of fluvial aggradation. Sedimentary dynamics was characterized by a higher frequency of flooding events affecting the arroyo's floodplain environment (Mehl and Zárate, 2012). This pattern was likely in connection with the onset of the Holocene climatic conditions at this latitudes (Zárate and Páez, 2002) driven by the general dynamics of the South American summer monsoon which progressively strengthened over the Holocene (Barros et al., 2002; Piovano et al., 2009; Garreaud et al., 2009; Vuille et al., 2012). Present-day dynamics indicate the formation during austral summer of a very deep continental low over the Chaco region (∼ 25° S, Fig. 1) forcing the easterly winds over the Amazon basin to be channeled southward between the eastern Andean slope and the Brazilian Plateau (Fig. 8a). The flow of low-level jet structure transports large amounts of moisture that feed convective summertime storms over the subtropical plains as far south as 35° S (Garreaud et al., 2009 and references therein). However, according to Barros et al. (2002), one of the two patterns of low-level flow and precipitation anomalies in Southern South America during midsummer (Fig. 8b and c) is associated with a main flow from the tropics turning eastwards towards the South Atlantic convergence zone (a diagonal band of precipitation maxima; Garreaud et al., 2009) and a westward anticyclonic circulation over southern Brazil, Paraguay and northern Argentina that turns south when reaching the Andes belt. It generates negative precipitation anomalies in northeastern Argentina and southern Brazil whereas positive anomalies are recorded in western Argentina favored by the transport of moisture from the Atlantic Ocean over the region (Fig. 8c) (Barros et al., 2002). Likely, during the early Holocene relatively heavy summer rainfalls generated by storms transporting moisture derived from the Atlantic could have affected the Andean piedmont area in similar conditions to the present ones.

Moisture differences at both side of the Andes south of the 35° S occur since the Lateglacial onwards (Piovano et al., 2009 and references therein; Markgraf et al., 2009). At the central Andean piedmont of Chile (∼ 32–45° S, Fig. 1) arid conditions dominating the early Holocene were attributed to substantially weaker Westerlies or latitudinally shifted westerly storm tracks in relation to a strengthened southeastern

CPD
9, 6125–6160, 2013

Pacific High (Jenny et al., 2002; Villa-Martínez et al., 2003; Markgraf et al., 2009, and references there in; Abarzúa et al., 2010). A marine pollen record located at 41° S suggest that the beginning of the early Holocene, at 10.7 cal kyr BP, was marked by warmer and dried conditions, a trend strengthened between 9.6 and 7.4 cal kyr BP (Montade et al., 2012).

Other LP–EH surface stabilization events can be found along the southern tip of South America. For example, at the piedmont plains of the Northwestern Pampean Ranges (Llanos de La Rioja, 29°57′ S and 65°52′ W, Fig. 1) a complex succession of environmental changes associated with four pedo-sedimentary cycles were recognized in likely Upper Pleistocene and Holocene deposits (Morrás et al., 2010). Further north, in the Bolivian Chaco (Fig. 1), a sensitive area to climatic change placed in the transition between the wet-climate Amazon basin and the subtropical semi-arid-climate Chaco, May et al. (2008) report evidence of late Quaternary paleoenvironmental changes in the paleosol–sediment sequences outcropping in the Grande river terraces. There, well developed Lateglacial paleosols document landscape geomorphological stability and wet conditions. Early Holocene likely palustrine sediments evidence flooding events into floodplain environments resulting from a significant increase in winter precipitation and, conversely, decreased summer precipitation (May et al., 2008). Between 11.2 and 8 cal ka BP the Bolivian Andes (Fig. 1) have record of paleowetlands formation (Servant and Servant-Vildary, 2003).

In the Pampas of Argentina, to the east of the SAAD (Fig. 1), the interfluve areas of the northern and eastern Pampas of Buenos Aires province (Fig. 1) have record of a paleosol (known as “Puesto Callejón Viejo” sensu Fidalgo et al., 1973) formed over Lateglacial sandy loess deposits (La Postrera Formation; Fidalgo et al., 1973) under a prevailing subhumid dry climate (Zárate et al., 2002). By the end of the late Pleistocene and the early Holocene loess aggradation dominated the undulating Pampa region (Pampa Ondulada, Fig. 1). Then, land surface stabilization gave way to the development of a paleosol that has remained at surface from then onwards (Kemp et al., 2006). On the other hand, fluvial basins of the main rivers of Pampas of Buenos Aires

CPD
9, 6125–6160, 2013

province record the development of a LP–EH paleosol on top of late Pleistocene alluvial sequences (Luján Formation; Fidalgo et al., 1973; Zárate et al., 2000; Prieto et al., 2004; Quatrocchio et al., 2008; Zech et al., 2009). In general terms, it has been inferred that Lateglacial conditions were dominated by channel and floodplain aggradation followed by pedogenesis during the LP–EH climatic transition. Then, the early-middle Holocene was featured by the occurrence of swampy environments associated to fluvial systems (shallow in-stream ponds) likely as a result of waterlogging within the river valleys. Bioclastic aggradation became dominant during the LP–EH transition and early Holocene in some fluvial basins (Zárate et al., 2000; Prieto et al., 2004). The observed paleoenvironmental changes have been linked to the prevalence of warmer and more humid climatic conditions in the Pampean plain (Muhs and Zárate, 2001; Zárate et al., 2000; Prieto et al., 2004). It has been pointed out that this climatic amelioration may have occurred in relation to a poleward shift of maritime tropical air masses and/or weakening of the South Atlantic anticyclone during the early and middle Holocene (Kemp et al., 2006; Quattrocchio et al., 2008, and references therein).

In North America, dark colored high- organic- sedimentary levels, "black mats", associated with Lateglacial–present Interglacial climatic transition has been reported at the very end of the Pleistocene at more than fifty geoarchaeological sites (Haynes, 1968, 2008; Firestone et al., 2007). Their formation have been related to the Younger Dryas cooling event. Firestone et al. (2007) linked this event to multiple meteorite impacts triggering a series of environmental catastrophes and biomass ignition resulting in the extinction of North American megafauna, major cultural changes and population decline among paleoindians. Nonetheless, Buchanan et al. (2008) and Marlon et al. (2009) deny such population decline and claim that biomass ignition was restricted and not related to major meteor impacts. However, Kennet et al. (2009) reinforce this controversy by indicating the existence of shock-synthesized hexagonal nanodiamonds associated to Ållerød–Younger Dryas Boundary sediments. In the Pampas of Argentina (Fig. 1), Toledo (2008) indicated the existance of "black mats" in the fluvial sequences of the

CPD
9, 6125–6160, 2013

Luján River and correlated them with those of North American endorsing the idea of a global climatic change.

6 Conclusions

This work contributes to the knowledge of the paleoenvironmental–paleoclimatic dominant conditions during the Lateglacial to early Holocene climatic transition in the eastern Andean piedmont between 33–34° S. There, the occurrence of a LP–EH transition paleosol records an interval of landscape geomorphological stability likely as a consequence of the climatic amelioration that followed the more arid climatic trend of the Lateglacial. Paleosol development was restricted to the alluvial basins of some arroyos crossing the Frontal Cordillera piedmont where it was preserved in the alluvial sequences. Paleosol poor development was closely related to the climatic conditions dominating the setting of the SAAD at that time. The onset at the early Holocene of more frequent flooding events in the eastern Andean piedmont could be linked to the influence of the South American Monsoon. Our observations are consistent with many other late Quaternary records from the southern tip of the South American, which collectively have evidence of alternating sedimentary-pedological processes by the end of the Pleistocene. The aridity pattern inferred for the Lateglacial in the eastern Andean piedmont was regionally widespread across the argentinian Pampean region where also a paleosol marks the transition to the most relative humid and warmer climatic conditions of the Holocene. In North America, the existence of LP–EH "black mat" deposits has been interpreted as a clear response to climate changes occurring during the Lateglacial–present Interglacial transition with a long-standing controversy around the likely triggering factors of that climatic change. In such a context, the occurrence of paleosols at the end of the Pleistocene is considered a suitable marker of a climatic event. We pose the importance of continuing unraveling the climatic changes that occurred during the transition from Lateglacial to present Interglacial conditions in the

CPD
9, 6125–6160, 2013

Andean piedmont. Geochemistry would be a plausible future exploratory line at the Late Quaternary alluvial sequences of Mendoza province.

Acknowledgements. This work was supported by CONICET and the National University of La Pampa, throughout projects PIP 5819 and EXA-186, respectively. Perla Imbellone is especially thanked for instructing A. Mehl in micromorphological analysis. We are grateful to Rob Kemp for kindly providing thin sections throughout "Argentinian loess paleosol records of past changes in climate" project. We expressed our gratitude to Leandro Rojo for helping during field work and to Hernán Ponce from the Dirección de Recursos Naturales de Tunuyán for providing logistic support.

References

Abarzúa, A. M., Adán, L., De Batist, M., and Maldonado, A.: Glacial to Holocene paleoclimate reconstruction based on laguna las Ranas record in south-central chile (39° S), in: Proceedings of the 18th International Sedimentological Congress, Mendoza, Argentina, 27 September–1 October 2010, abstracts CD-ROM, p. 91, 2010.

Abraham de Vázquez, E., Garleff, K., Liebricht, H., Regairaz, A., Schabitz, F., Squeo, F., Sting, H., Veit, H., and Villagrán, C.: Geomorphology and palaeocolgy of the Arid diagonal in the south America, edited by: Miller, H. and Hervé, F., Z. Angew. Geol., SH1, 55–61, 2000.

Azcuy, C. L.: Las secuencias sedimentarias neopaleozoicas, in: Geologí a y Recursos Naturales de Mendoza, edited by: Ramos, V. A., 12 °Congreso Geológico Argentino y 2 °Congreso de Exploración de Hidrocarburos, Mendoza, 10–15 October, I.5, 41–52, 1993.

Baker, V. R.: South American paleohydrology: future prospects and global perspective, Quaternary Int., 72, 3–5, 2000.

Barros, V. R. and Silvestri, G. E.: The relation between sea surface temperature at the subtropical south-central Pacific and precipitation in southeastern South America, J. Climate, 15, 251–267, 2002.

Barros, V., Doyle, M., González, M., Camilloni, I., Bejarán, R., and Caffera, R., Climate variability over subtropical South America and the South American monsoon: a review, Meteorologica, 27, 31–55, 2002.

Blasi, A., Zarate, M. A., and Kemp, B. M.: Sedimentación y pedogénesis cuaternaria en el noreste de la pampa bonaerense, LAJSBA, 8, 77–92, 2001.
Boninsegna, J., Argollo, J., Aravena, J. C., Barichivich, J., Christie, D., Ferrero, M. E., Lara, A., Le Quesne, C., Luckman, B. H., Masiokas, M., Morales, M., Oliveira, J. M., Roig, F., Srur, A., and Villalba, R.: Dendroclimatological reconstructions in South America: a review, Palaeogeogr. Palaeocl., 281, 210–228, 2009.
Buchanan, B., Collard, M., and Edinborough, K.: Paleoindian demography and the extraterrestrial impact hypothesis, P. Natl. Acad. Sci. USA, 105, 11651–11654, 2008.
Bullock, P., Fedoroff, N., Jongerius, A., Stoops, G., and Yursina, T.: Handbook for Soil Thin Section Description, Waine Research Publications, Wolverhampton, 152 pp., 1985.
Burgos, J. J. and Vidal, A. L.: Los climas de la República Argentina según la nueva clasificación de Thornwaite, Meteoros 1, 1–32, 1951.
Bruniard, E.: La diagonal árida Argentina: un límite climático real, Rev. Geogr. 95, 5–20, 1982.
Cabrera, A.: Regiones fitogeograficas Argentinas, in: Enciclopedia Argentina de Agricultura y Jardineria, fasciculo I, ACME Ed., Buenos Aires, 85 pp., 1976.
Caminos, R.: El basamento metamórfico Proterozoico-Paleozoico inferior, in: Geología y Recursos Naturales de Mendoza, edited by: Ramos, V. A., 12 Congreso Geológico Argentino y 2°Congreso de Exploración de Hidrocarburos, Mendoza, 10–15 October, I.2, 11–19, 1993.
Catt, J. A.: Paleopedology Manual, Quatern. Int., 6, 1–95, 1990.
Clapperton, C.: Quaternary Geology and Geomorphology of South America, Elsevier, Amsterdam, 779 pp., 1993.
Coronato, A. and Rabassa, J.: Late Quaternary in South America, in: Encyclopedia of Quaternary Science, edited by: Elias, S. A., Elsevier, Amsterdam, 1101–1109, 2007.
Espizua, L. E.: Glaciaciones Cuaternarias, in: Geología y Recursos Naturales de Mendoza, edited by: Ramos, V. A., 12 Congreso Geológico Argentino y 2 Congreso de Exploración de Hidrocarburos, Mendoza, 10–15 October, I.15, 195–203, 1993.
Espizua, L. E.: Quaternary glaciations in the Río Mendoza Valley, Argentine Andes, Quatern. Res. 40, 150–162, 1998.
Espizua, L. E.: Chronology of Late Pleistocene glacier advances in the Río Mendoza Valley, Argentina, Global Planet. Change, 22, 193–200, 1999.
Fidalgo, F., De Francesco, F., and Colado, U.: Geología superficial en las Hojas Castelli, J. M. Cobo y Monasterio (Pcia de Buenos Aires), in: Proceedings of the 5 Congreso Geológico Argentino, Carlos Paz, Córdoba, 22–28 October, 4, 27–39, 1973.

CPD
9, 6125–6160, 2013

Late Glacial-Holocene climatic transition

A. E. Mehl and M. A. Zárate

Firestone, R. B., Westc, A., Kennettd, J. P., Beckere, L., Bunchf, T. E., Revayg, Z. S., Schultzh, P. H., Belgyag, T., Kennetti, D. J., Erlandsoni, J. M., Dickensonj, O. J., Goodyeark, A. C., Harrish, R. S., Howardl, G. A., Kloostermanm, J. B., Lechlern, P., Mayewskio, P. A., Montgomeryj, J., Poredap, R., Darrahp, T., Que Heeq, S. S., Smith, A. R., Stichr, A., Toppings, W., Wittkef, J. H., and Wolbachr, W. S.: Evidence for an extraterrestrial impact 12,900 yr ago that contributed to the megafaunal extinctions and the Younger Dryas cooling, P. Natl. Acad. Sci. USA, 104, 16016–16021, 2007.

Frechen, M., Seifert, B., Sanabria, J. A., and Argüello, G. L.: Chronology of late Pleistocene Pampa loess from the Córdoba area in Argentina, J. Quaternary Sci., 24, 761–772, 2009.

Garreaud, R. D., Vuille, M., Compagnucci, R., and Marengo, J.: Present-day South American climate, Palaeogeogr. Palaeocl., 281, 180–195, 2009.

Haynes Jr., C. V.: Geochronology of a Late Quaternary alluvium, in: Means of Correlation of Late Quaternary Successions, edited by: Morrison, R. B. and Wright, H. E., Utah Press, Salt Lake City, 591–631, 1968.

Haynes Jr., C. V.: Younger Dryas “black mats” and the Rancholabrean termination in North America, P. Natl. Acad. Sci. USA105, 18, 6520–6525, 2008.

Imbellone, P. A. and Cumba, A.: Una sucesión con paleosuelos superpuestos en la zona sur de La Plata, Lajsba, 10, 1, 3–21, 2003.

Imbellone, P. A. and Teruggi, M. E.: Paleosols in loess deposits of the Argentine Pampa, Quaternary Int., 17, 49–55, 1993.

Jenny. B., Valero-Garcés, B. L., Villa-Martínez, R., Urrutia, R., Geyh, M., and Veit, H.: Early to Mid-Holocene ariditiy in Central chile and the southern westerlies: the laguna Aculeo record (34° S), Quaternary Res., 58, 160–170, 2002.

Kemp, R. A., Toms, P. S., Sayago, J. M., Derbyshire, E., King, M., and Wagoner, L.: Micromorphology and OSL dating of the basal part of the loess – paleosol sequence at La Mesada in Tucumán province, Northwest Argentina, Quaternary Int., 106/107, 111–117, 2003.

Kemp, R. A., King, M., Toms, P., Derbyshire, E., Sayago, J. M., and Collantes, M. M., Pedosedimentary development of part of a Late Quaternary loess – palaeosol sequence in Northwest Argentina, J. Quaternary Sci., 19, 567–576, 2004a.

Kemp, R. A., Toms, P. S., King, M., and Kröhling, D. M.: The pedosedimentary evolution and chronology of Tortugas, a Late Quaternary type-site of the northern Pampa, Argentina, Quaternary Int., 114, 101–112, 2004b.

Kemp, R. A., Zárate, M., Toms, P., King, M., Sanabria, J., and Arguello, G.: Late Quaternary paleosols, stratigraphy and landscape evolution in the Northern Pampa, Argentina, Quaternary Res., 66, 119–132, 2006.

Kennett, D., Kennett, J. P., West, A., West, G. J., Bunch, T. E., Culleton, B. J., Erlandson, J. M., Que Hee, S. S., Johnson, J. R., Mercer, C., Shen, F., Sellers, M., Stafford Jr., T. W., Stich, A., Weaver, J. C., Wittke, J. H., and Wolbach, W. S. Shock-synthesized hexagonal diamonds in Younger Dryas boundary sediments, P. Natl. Acad. Sci. USA, 106, 12623–12628, 2009.

Latrubesse, E. M.: The Late-Quaternary palaeohydrology of large South American fluvial systems, in: Palaeohydrology: Understanding Global Change, edited by: Gregory, K. J. and Benito, G., Wiley, Chichester, 193–212, 2003.

Llambías, E. J., Kleiman, L. E., and Salvarredi, J. E.: El magmatismo gondwánico, in: Geología y Recursos Naturales de Mendoza, edited by: Ramos, V. A., 12 Congreso Geológico Argentino y 2 Congreso de Exploración de Hidrocarburos, Mendoza, 10–15 October, I.6, 53–64, 1993.

Lee, J. A. and Kemp, R. A.: Thin sections of unconsolidated sediments and soils: a Recipe, in: Centre for Environmental Analysis and Management Technical Report, Department of Geography, Royal Holloway, University of London, London, UK, 1992.

Markgraf, V., Whitlock, C., Anderson, R. S., and García, A.: Late Quaternary vegetation and fire history in the northernmost Nothofagus forest region: Mallín Vaca Lauquen, Neuquén province, argentina, J. Quaternary Sci., 24, 248–258, 2009.

Marlon, J. R., Bartleina, P. J., Walsha, M. K., Harrisonb, S. P., Brown, K. J., Edwardse, M. E., Higuerag, P. E., Powerh, M. J., Andersoni, R. S., Brilesg, C., Brunelleh, A., Carcailletj, C., Danielsk, M., Hul, F. S., Lavoiem, M., Longn, C., Minckleyo, T., Richardp, P. J. H., Scottq, A. C., Shaferr, D. S., Tinners, W., Umbanhowar Jr., C. E., and Whitlockg, C.: Wildfire responses to abrupt climate change in North America, P. Natl. Acad. Sci. USA, 106, 8, 2519–2524, 2009.

May, J.-H., Zech, R., and Veit, H.: Late Quaternary paleosol–sediment-sequences and landscape evolution along the Andean piedmont, Bolivian Chaco, Geomorphology, 98, 34–54, 2008.

Mehl, A. E. and Zárate, M. A.: Late Quaternary alluvial records and environmental conditions in the eastern Andean piedmont of Mendoza (33–34° S, Argentina), J. S. Am. Earth Sci., 37, 41–59, 2012.

CPD

9, 6125–6160, 2013

Late Glacial-Holocene climatic transition

A. E. Mehl and M. A. Zárate

Montade, V., Combourier Nebout, N., Chapron, E., Mulsow, S., Abarzúa, A., Debret, M., Foucher, A., Desemt, M., Winiarski, T., and Kissel, C.: Regional vegetation and climate changes during the last 13 kyr from a marine pollen record in Seno Reloncaví, southern Chile, Rev. Palaeobot. Palyno., 181, 11–22, 2012.

Morrás, H., Moretti, L., Altinier, M. V., Favret, E., Bressan, E., and Romero, A.: First evidences of several pedo-sedimentary cycles in recent Quaternary sandy deposits in Los Llanos plains, La Rioja (Argentina), in: Proceedings of the 18th International Sedimentological Congress, Mendoza, Argentina, 27 September–1 October 2010, abstracts CD-ROM, p. 618, 2010.

Munsell Soil Color Charts: Munsell Color x-rite, Revised and washable version, Grand Rapids, X-Rite Incorporated, Michigan, USA, 2000.

Muhs, D. R. and Zárate, M.: Late quaternary eolian records of the Americas and their paleoclimatic significance, in: Interhemispheric Climate Linkages, edited by: Markgraf, V., Vol. 12, Academic Press, San Diego, 183–216, 2001.

Navarro, D.: Ambientes holocenos pedemontanos y de Montaña del sur de Mendoza, Ph.D thesis, Universidad Nacional de Mar del Plata, Buenos Aires, Argentina, 2012.

Piovano, E., Damatto Moreira, S., and Ariztegui, D.: Recent environmental changes in Laguna Mar Chiquita (Central Argentina): a sedimentary model for a highly variable saline lake, Sedimentology, 49, 1371–1384, 2002.

Piovano, E. L., Ariztegui, D., Córdoba, F., Cioccale, M., and Sylvestre, F.: Hydrological variability in South America below the Tropic of Capricorn (Pampas and Patagonia, Argentina) during the last 13.0 ka, in: Past Climate Variability in South America and Surrounding Regions (Developments in paleoenvironmental research), edited by: Vimeux, F., Sylvestre, F., and Khodri, M., Springer, New York, 14, 323–351, 2009.

Polanski, J.: Estratigrafía, neotectónica y geomorfología del Pleistoceno pedemontano entre los ríos Diamante y Mendoza, Revista De La Asociación Geológica Argentina, 17, 3/4, 127–349, 1963.

Prieto, A. R.: Late Quaternary vegetational and climatic changes in the pampa grassland of Argentina, Quaternary Res., 45, 1, 73–88, 1996.

Prieto, A., Blasi, A., De Francesco, C., and Fernández, C.: Environmental history since 11,000 ^{14}C yr B. P. of the northern Pampas, Argentina from alluvial sequences of the Luján River, Quaternary Res. 62, 2, 146–161, 2004.

CPD
9, 6125–6160, 2013

A. E. Mehl and M. A. Zárate

Prieto, M. R., Villagra, P. E., Lana, N. B., and Abraham, E. M.: Utilización de documentos históricos en la reconstrucción de la vegetación de la Llanura de la Travesía (Argentina) a principios del siglo XIX, Rev. Chil. Hist. Nat., 76, 4, 613–622, 2003.

Prohaska, F. J.: Las características de las precipitaciones en la región semiárida pampeana, Revista De Investigaciones Agronómicas, 15, 199–232, 1961.

Quattrocchio, M. E., Borromei, A. M., Deschamps, C. M., Grill, S. C., and Zavala, C. A.: Landscape evolution and climate changes in the Late Pleistocene–Holocene, southern Pampa (Argentina): evidence from palynology, mammals and sedimentology, Quaternary Int., 181, 123–138, 2008.

Rabassa, J.: Late Cenozoic Glaciations in Patagonia and Tierra del Fuego, in: The Late Cenozoic of Patagonia and Tierra del Fuego, edited by: Rabassa, J., Developments in Quaternary Sciences, Elsevier, Amsterdam, 11, 151–204, 2008.

Roig, F. A. and Martínez Carretero, E.: La vegetación puneña en la provincia de Mendoza, Argentina, Phytocenologia, 28, 565–608, 1998.

Rojo, L. D., Mehl, A. E., Paez, M. M., and Zárate, M.A: Mid- to Late Holocene pollen and alluvial record of the arid Andean piedmont between 33° and 34° S, Mendoza, Argentina: inferences about floodplain evolution, J. Arid Environ. 77, 110–122, 2012.

Saltzman, B.: Dynamical Paleoclimatology, Generalized Theory of Global Climate Change, International Geophysics Series, Vol. 80, Academic Press, New York, London, 392 pp., 2002.

Schaetzl, R. and Anderson, S.: Soils, Genesis and Geomorphology, Cambridge University Press, Cambridge, 817 pp., 2005.

Servant, M. and Servant-Vildary, S.: Holocene precipitation and atmospheric changes inferred from river paleowetlands in the Bolivian Andes, Palaeogeogr. Palaeocl., 194, 187–206, 2003.

Soil Survey Staff: Soil Taxonomy: a Basic System of Soil Classification for Making and Interpreting Soil Surveys, Natural Resources Conservation Service, 2nd Edn., US Department of Agriculture, Washington, D.C., 870 pp., 1999.

Soil Survey Staff: Keys to Soil Taxonomy, Natural Resources Conservation Service, 9th Edn., US Department of Agriculture, Washington, D.C., 334 pp., 2003.

Sruoga, P., Llambías, E. J., Fauqué, L., Schonwandt, D., and Repol, D. G.: Volcanological and geochemical evolution of the Diamante Caldera – Maipo Volcano Complex in the southern Andes of Argentina (34°10′ S), J. S. Am. Earth Sci., 19, 4, 401–406, 2005.

CPD
9, 6125–6160, 2013

Teruggi, M. E. and Imbellone, P. A. Paleosuelos loéssicos superpuestos en el Pleistoceno superior – Holoceno de la región de La Plata. Provincia de Buenos Aires, Argentina, Ciencia Del Suelo, 5, 175–188, 1987.

Toledo, M. J.: La crisis climática de 13.000 AP: "mantos negros", extinciones de megafauna y cambios poblacionales, in: Proceedings of the 17°Congreso Geológico Argentino, San Salvador de Jujuy, 7–10 October, 735–736, 2008.

Toms, P. S., King, M., Zárate, M. A., Kemp, R. A., and Foit Jr., F. F.: Geochemical characterization, correlation, and optical dating of tephra in alluvial sequences of central western Argentina, Quaternary Res., 62, 60–75, 2004.

Tripaldi, A. and Forman, S. L.: Geomorphology and chronology of Late Quaternary dune fields of western Argentina, Palaeogeogr. Palaeocl., 251, 300–320, 2007.

Tripaldi, A., Zárate, M. A., and Brook, G. A., Li, G.-Q.: Late Quaternary paleoenvironments and paleoclimatic conditions in the distal Andean piedmont, southern Mendoza, Argentina, Quaternary Res., 76, 2, 253–263, 2011.

Tucker, M. E.: Sedimentary Rocks in the Field, 3rd edn., John Wiley & Sons Ltd, Chichester, 234 pp., 2003.

Villalba, R.: Climatic fluctuations in northern Patagonia during the last 1000 yr as inferred from tree-ring records, Quaternary Res., 34, 3, 346–360, 1990.

Villa-Martínez, R., Villagrán, C., and Jenny, B.: The last 7500 cal yr B. P. of westerly rainfall in Central Chile inferred from a high-resolution pollen record from Laguna Aculeo (34° S), Quaternary Res., 60, 284–293, 2003.

Vuille, M., Burns, S. J., Taylor, B. L., Cruz, F. W., Bird, B. W., Abbott, M. B., Kanner, L. C., Cheng, H., and Novello, V. F.: A review of the South American monsoon history as recorded in stable isotopic proxies over the past two millennia, Clim. Past, 8, 1309–1321, doi:10.5194/cp-8-1309-2012, 2012.

Yrigoyen, M.: Los depósitos sinorogénicos terciarios, in: Geología y Recursos Naturales de Mendoza, Ramos, V. A. (Ed.). 12°Congreso Geológico Argentino y 2°Congreso de Exploración de Hidrocarburos, Mendoza, 10–15 October, I.17, 217–234, 1993.

Zárate, M. A. and Mehl, A.: Estratigrafía y geocronología de los depósitos del Pleistoceno tardío/Holoceno de la cuenca del Arroyo La Estacada, departamentos de Tunuyán y Tupungato (Valle de Uco), Mendoza, Revista De La Asociación Geológica Argentina, 63, 407–416, 2008.

Zárate, M. A. and Páez, M. M.: Los paleoambientes del Pleistoceno tardío-Holoceno en la cuenca del Arroyo La Estacada, Mendoza, in: IANIGLA, 30 años de investigación básica y aplicada en ciencias ambientales, edited by: Trombotto, D. and Villalba, R., Ianiglia, Mendoza, 117–121, 2002.
Zárate, M. A., Kemp, R. A., Espinoza, M., and Ferrero, L.: Pedosedimentary and palaeoenvironmental significance of a Holocene alluvial sequence in the southern Pampas, Argentina, Holocene, 10, 4, 481–488, 2000.
Zárate, M. A., Kemp, R. A., and Blasi, A. M.: Identification and differentiation of Pleistocene paleosols in the northern Pampas of Buenos Aires, Argentina, J. S. Am. Earth Sci., 15, 303–313, 2002.
Zech, W., Zech, M., Zech, R., Peinemann, N., Morrás, H. J. M., Moretti, L., Ogle, N., Kalim, R. M., Fuchs, M., Schad, P., and Glaser, B.: Late Quaternary palaeosol records from subtropical (38° S) to tropical (16° S) South America and palaeoclimatic implications, Quaternary Int., 196, 107–120, 2009.

CPD
9, 6125–6160, 2013

A. E. Mehl and M. A. Zárate

Table 1. Arroyo La Estacada basin alluvial record: lithostratigraphic description and interpretation of lithofacies (from Mehl and Zárate, 2012).

Lithofacies	Description	Interpretation
Sr	Ripple cross – laminated fine sand, silty sand and sandy silt.	Subaqueous migration of trains of ripples with a low rate of sedimentation from suspension leading to mutually erosive ripples.
Src	Climbing ripple cross–laminated fine sand, silty sand or sandy silt.	Subaqueous migration of trains of ripples and addition of sediment from suspension leading to partial preservation of the ripple stoss sides and climbing of the ripple train.
Sm	Massive sand, silty sand or sandy silt, scarcely coarse sand grains dispersed. Horizontal and laterally continuous, beds of variable thick.	Fluid flows. Secondary weathering process could affect the structure of deposits.
Sme	Well selected, massive or diffuse horizontal laminated fine sand or silty fine sand.	Aeolian ripple migration or vertical aggradation in a partially vegetated sandy blanket.
Fl	Horizontal laminated sand, silty sand, sandy silt, silt or clay. Interbedded silt and clay.	Deposition from a suspension and sometimes deposition from weak traction currents in overbank areas.
Fm	Massive silt – clay. Occasionally with bioturbation and features of pedogenesis. Also, thin mud drapes develop over gravel, sandy gravels and sand.	Deposition from a suspension and likely later bioturbation and pedogenesis.
Fsm	Horizontal laminated silt, clay, clayey silt or silty clay.	Deposition from a suspension in distal overbank areas.
C	Organic charcoal in sediments. Dark to very dark colors and abundant organic matter content. Abrupt upper and lower limits. Sometimes laterally continues for several meters.	Deposition of organic matter either transported in water suspension or derived from floating aquatic plants. Also, plant fragments accumulation in a swampy environment.
Pa	Alluvial sedimentary deposits with development of pedological features.	Pedogenetic processes develop in overbank sedimentary deposits with abundant vegetation and sometimes waterlogged.
Psme	Aeolian massive or horizontal laminated fine sand and silty sand, with development of pedological features.	Pedogenetic processes affecting aeolian deposits.
P	Nodules and concretions of variable form and size.	Pedogenetic process, shallow water evaporation in overbank areas or mineral-bearing water movement throughout alluvial deposits.
D	Moderate to highly indurate sediments (hardened crust). Cements could be formed by calcium carbonate and/or sulfates (e.g. gypsum).	Accumulation of chemically precipitated soluble salts from mineral-bearing water likely moving upward by capillary action, then evaporated during dry seasons.

CPD
9, 6125–6160, 2013

Table 2. Late Pleistocene–Holocene transition paleosol: horizonation, structure, air-dried color sample (Munsell Soil Color Chart, 2000), limits, organic matter (OM)-calcium carbonate ($CaCO_3$) contents, and radiocarbonic ages at the three involved study sites. Calibrated radiocarbon ages: Calib 6.1.0 Program, 2 sigma standard deviation. (*) SH calibration curves are not valid to calibrate this age.

Study Site	Horizon	Structure	Munsell Color	Limit		OM %	$CaCO_3$ %	Radiocarbon Ages					
				Upper	Lower			Lab No	Material	^{14}C Age (BP)	$\delta^{13}C$	Calibrated Age (2Δ)	Author
Puente el Zampal	A	Massive	10 YR 6/1– 10 YR 6/2	Smooth and abrupt	Very irregular and gradual	1.33	0.2	NSRL–12 644	OM	2990 ± 30	−15.0	2967–3211 (p: 1)	Zárate and Mehl (2008)
								Beta-135581	OM	7890 ± 50	−25.0	8454–8968 (p: 0.96) 8832–8862 (p: 0.022) 8890–8890 (p: 0.0004) 8919–8952 (p: 0.019) 8964–8968 (p: 0.002)	Zárate and Mehl (2008)
	C		10 YR 6/2			0.40	1.20	Beta-135580	OM	9420 ± 60	−25.0	10 303–10 314 (p: 0.005) 10 391–10 753 (p: 0.995)	Zárate and Mehl (2002)
								Beta-135579	OM	9610 ± 60	−25.0	10 685–11 144 (p: 1)	Zárate and Mehl (2002)
								NSRL-12643	OM	10 250 ± 40	−15.8	11 709–12 075 (p: 1)	Mehl and Zárate (2012)
								Beta-154137	OM	17 110 ± 70	−21.0	*Calibration curve is not valid*	Zárate and Páez (2002)
Puente Roto	A	Massive	10 YR 6/2	Smooth and clear	Smooth and gradual	1.95– 1.34	1.30– 1.80	NSRL-12645	Molusc shell	7450 ± 40	−6.4	8050–8093 (p: 0.058) 8106 — 8119 (p: 0.012) 8133–8139 (p: 0.005) 8155–8345 (p: 0.92)	This paper
	Ck or Bk?		10 YR 8/3			0.35	15.60	Beta-154136	OM	10 090 ± 50	−18.3	11 275–11 770 (p: 0.99) 11 790–11 805 (p: 0.007)	This paper
Finca Gatica	A	Massive	10 YR 6/2	Smooth and abrupt	Smooth and diffuse	0.13	2.5	–					
	C		10 YR 6/2			0.27	3.1						

CPD
9, 6125–6160, 2013

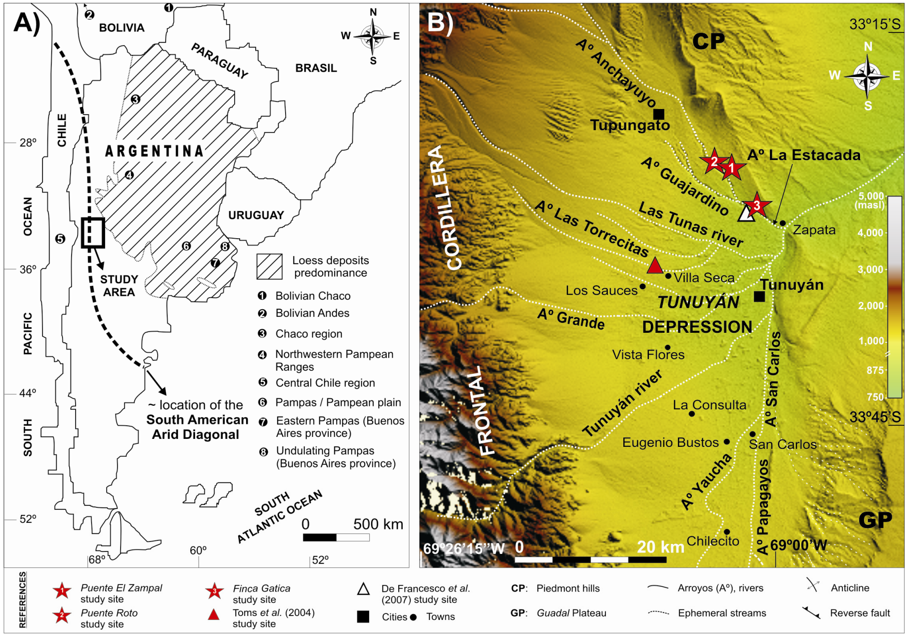

Fig. 1. (A) Location map. Approximate distribution of loess deposits in Argentina (Zinck and Sayago, 1999) and extension of the South American Arid Diagonal. **(B)** Digital elevation model and fluvial drainage at the eastern Andean piedmont between 33–34° S, Mendoza province, Argentina.

CPD
9, 6125–6160, 2013

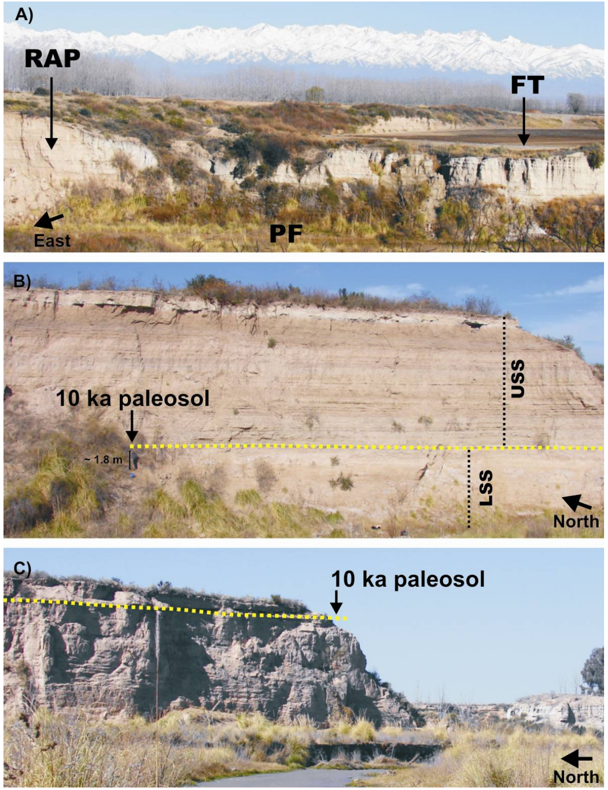

Fig. 2. Late Pleistocene–Holocene alluvial sequence at Arroyo La Estacada. **(A)** View of the three geomorphological units differentiated at the arroyo valley: regional aggradational plain (RAP), fill terrace (FT) and present floodplain (PF) (Zárate, 2002; Zárate and Mehl, 2008). **(B)** Puente El Zampal study site: RAP unit at the cut bank of Arroyo Anchayuyo; lower and upper stratigraphic sections (LSS, USS) are shown. **(C)** RAP at Finca Gatica study site, Arroyo La Estacada.

CPD
9, 6125–6160, 2013

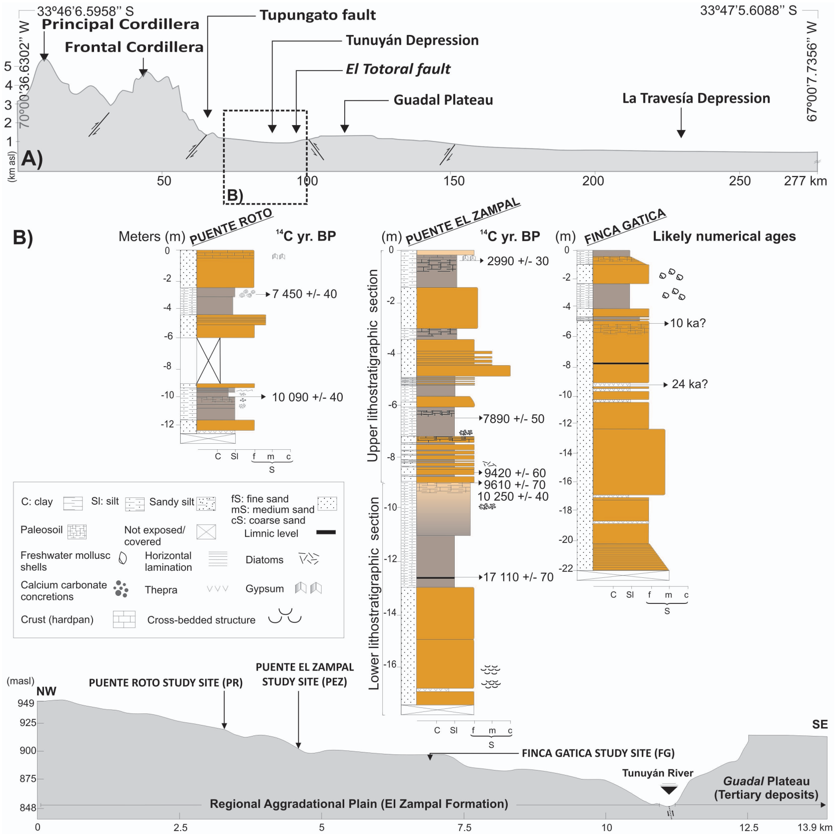

Fig. 3. (A) Sketch showing the main morphostrucutral units of the Frontal cordillera piedmont at the study area (vertical scale is exaggerated). Tunuyán Depression study area is boxed. **(B)** Schematic topographic profile (adapted from Google Earth software) along the Regional Aggradational Plain in the vicinities of the arroyos Anchayuyo and La Estacada riverbanks. Lithostratigrapic field logs at each study site are shown.

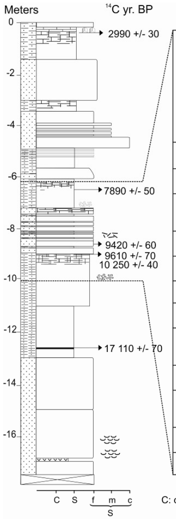

Sample	Depth in profile (m)	Microstructure	Voids		G/F_{62}	B -fabric	Crystalline pedofeatures	Excremental nfillings	Clay coatings	Fe-Mn concentration features				Calcitic concentration features (micrite)		Organic matter		Diatoms
			Total (%)	Type						Nodules	Hypo-coatings	Quasi-coatings	Diffusion	Nodules	Cements	Plant residues	Organic punctuations	
PEZ 1	7.35 - 9.00	m	40	Cr,C, Ch	60 - 40	En	--	--	--	--	--	--	--	--	--	**** (5%)	--	--
PEZ 2		m	30	Cr, C	10 - 90	cS	**** (10%)	--	--	***	--	**	--	**	--	***	**	***
PEZ 3		m	30	Cr,C, Ch	10 - 90	cS, M	**** (10%)	**	--	**** (10%)	--	--	**** (15 %)	--	--	**** (10%)	**	--
PEZ 4		a b	20	Cr,C, Ch	2 - 98	cS	**** (10%)	--	--	--	***	--	***	--	***	***	**** (15%)	***
PEZ 5		m	20-30	Cr, C, Ch	20 - 80	--	--	--	--	--	--	--	***	--	--	**	***	--
PEZ 6		m	2-5	Cr	10 - 90	M	--	**	*	**	***	--	****	--	--	***	**	***
PEZ 7		m	10	Cr, C	5 - 95	--	***	***	**	**	*	--	--	**** (10%)	--	***/*** *	--	**** (5-10%)
PEZ 8	9 - 9.35	m	5-20	Cr,C, Ch	30 - 70	rS, cS,U	--	*	--	--	--	--	--	***	**** (5 - 10%)	***	--	--
PEZ 9		m-s	2-20	C,Ch	70 - 30	M	--	--	--	--	--	--	--	--	**** (10%)	--	--	--
PEZ 10	9.35 - 10	m	<5	C, Cr	80 - 20	--	--	**	--	--	--	--	**** (10%)	--	**** (30%)	--	--	--
PEZ 11		m-s	<5-10	C, Ch, V	60 - 40	--	--	**	--	**	--	--	-	***	**** (50%)	--	--	--
PEZ 12		m - s	10-20	C, Ch	15 - 85	C,M	**	--	--	**	**	**	***	**	***	--	--	--

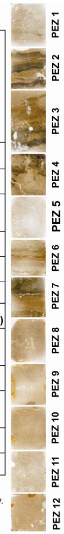

C: clay. S: silt. Sandy silt. Calcium carbonate concretions. Crust (hardpan). Limnic level. Cross-bedded structure. **m**: massive. **p**: prismatic. **s**: spongy.
S: Sand; (f) fine sand, (m) medium, (c) coarse. Paleosoil. Gypsum. Not exposed/covered. Diatoms. **ab**: blocky (angular blocks). **G/F_{62}**: coarse/fine relation. **C**: channels.
Ch: chambers. V: vughs. **Cr**: cracks. **M**: mosaic-speckled. **cS**: cross-striated. **rS**: reticulate striated. **U**: unistral. **C**: crystallitic. **En**: enaulic. - not detected. * rare (<0.2%). ** (0.2-2%). *** few (>2-5%). **** common (>5%). p: percentile.

Fig. 4. Alluvial sequence field log at Puente El Zampal study site (Arroyo Anchayuyo) and micromorphology of the ca. 10 ka paleosol.

CPD
9, 6125–6160, 2013

CPD
9, 6125–6160, 2013

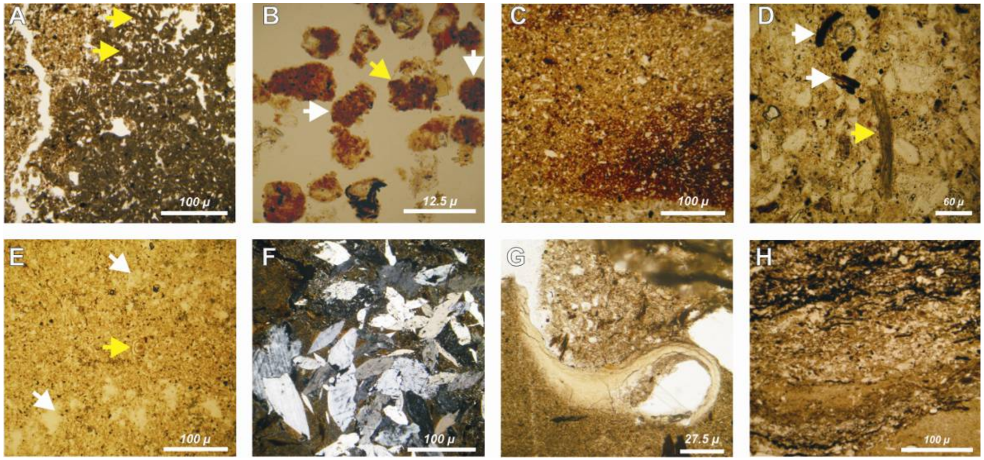

Fig. 5. Puente El Zampal locality: photomicrographs of micromorphological features (PPL: plane polarized light. XPL: crossed polarized light). **(A)** Calcitic concentration feature and spongy microstructure (arrows) (Sample: PEZ 12, PPL). **(B)** Spherical, bacillo-cylinder (white arrows) and irregular (yellow arrow) excrement pedofeatures infilling a void (Sample: PEZ 11, PPL). **(C)** Ferruginous impregnation in the soil mass (Sample: PEZ 10, PPL). **(D)** Unidentified particles of organic matter (white arrows) and a tissue residue (yellow arrow) (Sample: PEZ 8, PPL). **(E)** Concentric clay coating in a void (yellow arrow) and spongy microstructure in the bottom/right upper areas of the thin section (white arrows) (Sample: PEZ 9, PPL). **(F)** Gypsum crystal aggregate (Sample: PEZ 4, XPL). **(G)** Chamber clayed-infill (Sample: PEZ 11, PPL). **(H)** Plant residues included into different grain size sedimentary layers (Sample: PEZ 2, PPL).

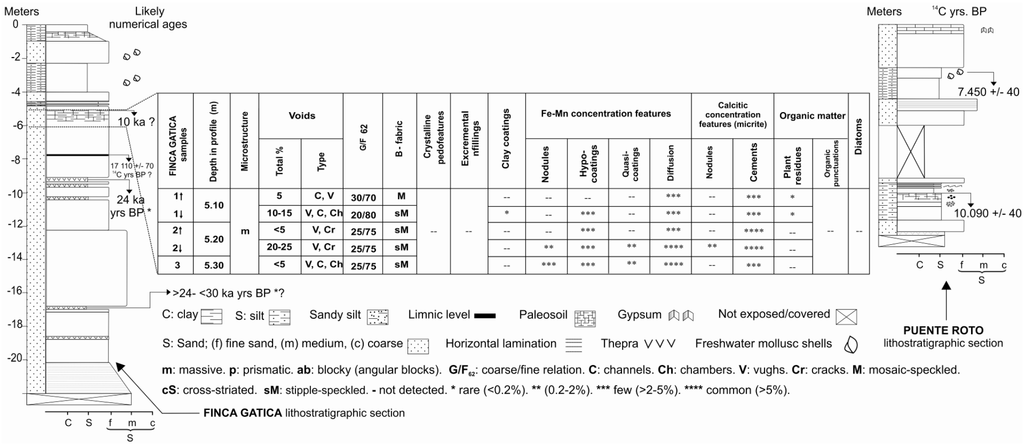

FINCA GATICA samples	Depth in profile (m)	Microstructure	Voids: Total %	Voids: Type	G/F 62	B - fabric	Crystalline pedofeatures	Excremental nfillings	Clay coatings	Fe-Mn concentration features: Nodules	Fe-Mn: Hypo-coatings	Fe-Mn: Quasi-coatings	Fe-Mn: Diffusion	Calcitic concentration features (micrite): Nodules	Calcitic: Cements	Organic matter: Plant residues	Organic matter: Organic punctuations	Diatoms
1↑	5.10	m	5	C, V	30/70	M	--	--	--	--	--	--	***	--	***	*	--	--
1↓			10-15	V, C, Ch	20/80	sM			*	--	***	--	***	--	***	*		
2↑	5.20		<5	V, Cr	25/75	sM			--	--	***	--	***	--	****	--		
2↓			20-25	V, Cr	25/75	sM			--	**	***	**	****	**	****	--		
3	5.30		<5	V, C, Ch	25/75	sM			--	***	***	**	****	--	***	--		

Fig. 6. Alluvial sequence field log at Finca Gatica study site (Arroyo La Estacada) and micromorphology of the ca. 10 ka paleosol. A field log in Puente Roto study site (Arroyo Anchayuyo) is also schematized.

CPD
9, 6125–6160, 2013

Late Glacial-Holocene climatic transition

A. E. Mehl and M. A. Zárate

Title Page
Abstract Introduction
Conclusions References
Tables Figures
◀| |▶
◀ ▶
Back Close
Full Screen / Esc
Printer-friendly Version
Interactive Discussion

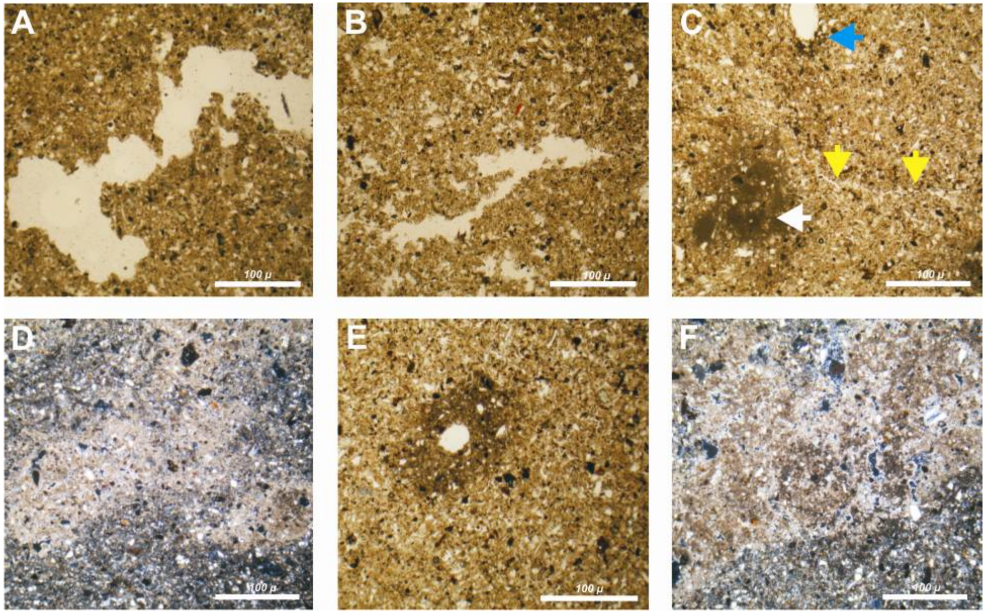

Fig. 7. Finca Gatica locality: photomicrographs of micromorphological features (PPL: plane polarized light. XPL: crossed polarized light). **(A, B)** Chambers with mamillate surface roughness. Microphotograph B also shows zones with spongy-like structure (Samples: FG 1 and FG 2, PPL). **(C)** Calcitic impregnation (white arrow), slight hypocoating and calcitic diffusion around a void (light blue arrow) and a crack (yelloow arrows) (Sample: FG 2, XPL). **(D)** Calcitic diffusion in the soil mass (Sample: FG 1, PPL). **(E)** Calcitic hypocoating and diffusion around a void (Sample FG 1, PPL). **(F)** Calcitic diffusion in the soil mass (Sample: FG 2, XPL).

CPD
9, 6125–6160, 2013

Late Glacial-Holocene climatic transition

A. E. Mehl and M. A. Zárate

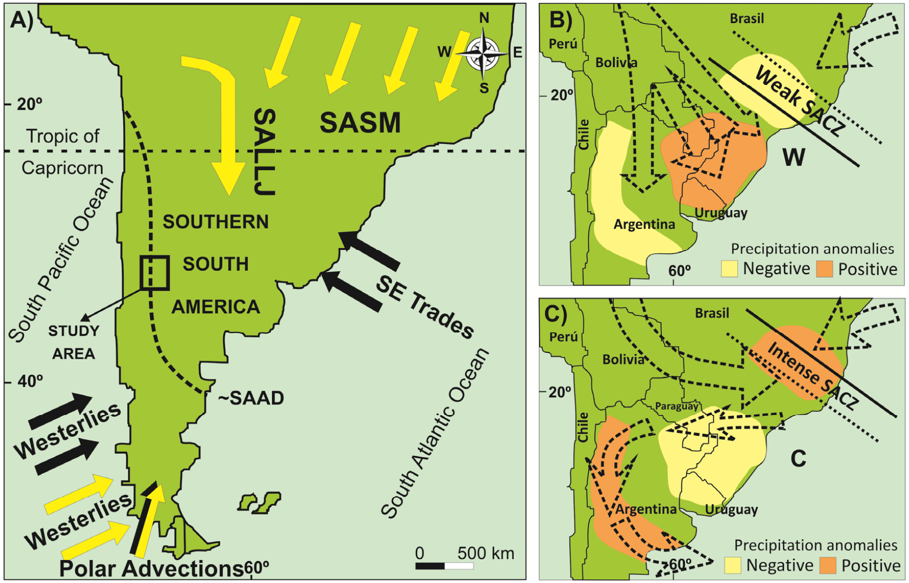

Fig. 8. (A) Main components of the seasonal atmospheric circulation patterns in southern South America adapted from Piovano et al. (2009). SASM: South American Summer Monsoon. SALLJ: South American Low Level Jets. Dashed-line: approximate location of the South American Arid Diagonal. Yellow arrows: austral summer. Black arrows: austral winter. (**B** and **C**) Scheme of the two low-level circulation and precipitation main midsummer patterns at southern South America from Barros et al. (2002). Regions of positive (negative) precipitation anomalies are orange-shaded (yellow-shaded). Dashed line: approximate mean axis of the convective activity in the SACZ and in its continental extension.